The Carotenoid S_1 State in LH2 Complexes from Purple Bacteria *Rhodobacter sphaeroides* and *Rhodopseudomonas acidophila*: S_1 Energies, Dynamics, and Carotenoid Radical Formation

Tomáš Polívka,*,† Donatas Zigmantas,† Jennifer L. Herek,† Zhi He,† Torbjörn Pascher,† Tõnu Pullerits,† Richard J. Cogdell,‡ Harry A. Frank,§ and Villy Sundström†

Chemical Physics, Lund University, Box 124, S-221 00 Lund, Sweden, Division of Biochemistry and Molecular Biology, Institute of Biomedical Sciences, University of Glasgow, G12 8QQ Glasgow, U.K., and Department of Chemistry, University of Connecticut, Storrs, Connecticut 0629−3060

Received: March 12, 2002; In Final Form: July 16, 2002

Using near-infrared femtosecond absorption spectroscopy, we have determined the S_1 energies of the carotenoids spheroidene and rhodopin glucoside in LH2 complexes of purple bacteria. The S_1 energies in the LH2 complexes yield values of 13400 ± 100 cm^{-1} for spheroidene and 12550 ± 150 cm^{-1} for rhodopin glucoside, which are very close to the S_1 energies obtained for both carotenoids in solution. The 850 cm^{-1} difference between the S_1 energies of these two carotenoids significantly affects the energy transfer pathways within the LH2 complexes. The S_1 energy of spheroidene in the LH2 complex of *Rhodobacter* (*Rb.*) *sphaeroides* is high enough to allow efficient energy transfer from the S_1 state to bacteriochlorophylls, resulting in a substantial shortening of the spheroidene S_1 lifetime in the LH2 complex (1.7 ps) compared with the lifetime in solution (8.5 ps). Rhodopin glucoside, which occurs in *Rhodopseudomonas* (*Rps.*) *acidophila*, has an S_1 energy in the LH2 complex too low for efficient S_1-mediated energy transfer and therefore the S_2 state becomes the main energy donor in LH2 complexes containing this carotenoid. In addition, a distinct carotenoid spectral band not observed in solution, was detected at around 960 nm in the LH2 complex of *Rb. sphaeroides*. This band is assigned to a spheroidene radical cation, which is formed in ∼200 fs and decays within 8 ps. The yield of the spheroidene radical formation is estimated to be in the range of 5−8%.

1. Introduction

Carotenoids are a class of natural pigments that play important roles in several biological systems. Their functions are probably best understood in photosynthetic organisms where they serve as light-harvesting pigments together with (bacterio)chlorophylls (BChls).[1] Many photosynthetic systems also rely on carotenoids to quench (B)Chl triplet states.[2] Efficient quenching of singlet oxygen or reactive radicals by carotenoids is thought to be an important function in a variety of living organisms including humans.[3] The bright colors of carotenoids varying from yellow to red are due to their strong absorption bands (extinction coefficients on the order of 10^5) in the 400−550 nm spectral region.[4] In this region BChls are not very good absorbers, enabling carotenoids to assist in the light-harvesting process.

One of the important pieces of information for understanding of spectroscopic properties of carotenoids is the symmetry of the conjugated backbone of the molecule, which is approximated by the C_{2h} point symmetry group. Although carotenoids do not exhibit perfect C_{2h} symmetry, many of their photophysical properties can be understood on the basis of polyenes possessing ideal C_{2h} symmetry.[5] In this context, the strong absorption of carotenoids in the 400−550 nm region is due to a transition from the ground state S_0 ($1A_g^-$) to the second excited state S_2 ($1B_u^+$), while the lowest lying excited state S_1 ($2A_g^-$) has the same symmetry as the ground state and hence the S_0-S_1 transition is forbidden.[4] It is important to note that here we denote the $1B_u^+$ state as S_2 although evidence is accumulating that other states, which are not accessible from the ground state, can exist between the S_1 and S_2 states.[6,7]

The light-harvesting function of carotenoids relies on their ability to transfer energy efficiently from the low-lying excited states to (B)Chls. It was shown for a number of light-harvesting systems that carotenoids are able to transfer energy directly from both S_1 and S_2 states with various efficiencies according to the particular donor and acceptor molecules involved in the process.[8−12] A number of experimental[7−12] and theoretical[13−17] investigations have shown that an understanding of the pathways and mechanisms of carotenoid-(B)Chl energy transfer requires a precise knowledge of the spectroscopic properties of the pigments involved. Since energy transfer involves both the S_2 and S_1 states, it is clear that a detailed understanding of the properties of these states is required. While the lifetime of the S_1 state can be measured via the S_1-S_N transient absorption occurring in the visible spectral region,[18] the energy of the S_1 state, which is one of the most important parameters controlling energy transfer processes between carotenoids and (B)Chls, cannot be easily obtained by conventional spectroscopic methods.

A substantial effort has been made to determine the energy of the S_1 state in solution using experimental approaches based on resonance Raman,[19,20] fluorescence,[21−23] or near-infrared femtosecond transient absorption spectroscopy.[24,25] However, to understand the relevance of the S_1 state to the process of

* Corresponding author. E-mail: tomas.polivka@chemphys.lu.se. Fax: +46−46−222 4119.
† Chemical Physics.
‡ Institute of Biomedical Sciences.
§ Department of Chemistry.

10.1021/jp025752p CCC: $22.00
Published on Web 09/28/2002

energy transfer, it is necessary to determine the S_1 energy of carotenoids in their natural protein environment. Two experimental approaches toward achieving this goal were recently developed. One is based on a two-photon absorption technique which was used to obtain the S_1 energy of the carotenoid, spheroidene, in the LH2 light-harvesting complex of purple bacteria.[26,27] The two-photon technique employs BChl*a* fluorescence for detection, and therefore generates an excitation spectrum. This spectrum does not necessarily reveal the lowest 0−0 vibronic transition of the carotenoids, as was demonstrated recently for carotenoids in the LHCII antenna complex from higher plants.[28] An alternate experimental approach to determine the S_1 energies of carotenoids is based on measurements of the S_1-S_2 excited state absorption (ESA) detected shortly after excitation.[24] In contrast to the S_0-S_1 transition, the S_1-S_2 transition is allowed according to the symmetry selection rules. By scanning the probe wavelength within the time window given by the S_1 lifetime in the near-infrared region, one can obtain a spectral profile of the S_1-S_2 transition and determine the energy gap between the 0−0 transitions of the S_1 and S_2 states. From the energies of the S_1-S_2 and S_0-S_2 transitions, the S_1 energy can be deduced by subtraction. This method was used to obtain S_1 energies of a few carotenoids in solution,[12,24,25] and as shown recently for xanthophylls in the LHCII antenna complex from higher plants,[29] there are no restrictions to this method in obtaining the S_1 energies of carotenoids in the protein environment.

To extend this study to other light-harvesting complexes, we have chosen the LH2 light-harvesting antenna complexes from the purple bacteria *Rhodobacter* (*Rb.*) *sphaeroides* and *Rhodopseudomonas* (*Rps.*) *acidophila*. Extensive knowledge of photochemistry of these complexes has been accumulated,[30] and in contrast to the LHCII antenna complex, the absorption bands of carotenoids and BChls are well resolved and separated, which simplifies the experiment. In addition, the structure of *Rps. acidophila* has been resolved to 2.4 Å resolution,[31] which was very recently refined to 2.0 Å,[32] revealing the positions of the pigments within the LH2 complex. Although the X-ray structure of the LH2 complex from *Rb. sphaeroides* has not been reported, cryo-electron microscopy studies suggest that the structure of this LH2 complex is likely to be similar to the one from *Rps. acidophila*.[33] Both complexes exhibit 9-fold symmetry and contain 27 BChl*a* and 9 carotenoid molecules arranged in a ring with its axis perpendicular to the membrane plane. Elementary building blocks of LH2 complexes are $\alpha\beta$-polypeptide pairs that bind two strongly coupled BChl*a* molecules absorbing at around 850 nm (B850), one BChl*a* molecule having an absorption band at 800 nm (B800), and one carotenoid molecule spanning the membrane in close contact with both the B800 and B850 molecules (Figure 1). The key difference between the complexes is that the LH2 complex from *Rb. sphaeroides* contains the carotenoid spheroidene, having 10 conjugated C═C bonds, while *Rps. acidophila* LH2 contains the carotenoid rhodopin glucoside (RG), which has a conjugated chain length of 11. This distinction leads to dramatic consequences regarding energy transfer pathways within the LH2 complexes.

Investigations comparing light-harvesting complexes from purple bacteria containing different carotenoids have established that the conjugation length of the carotenoid is a crucial factor governing whether the S_2 or S_1 state is the primary route of energy transfer.[8,9,34] For carotenoids having 11 or more conjugated C═C bonds, the S_1 state is thought to be too low for efficient energy transfer to BChls. Decreasing the conjugation length, however, shifts the S_1 energy high enough to produce

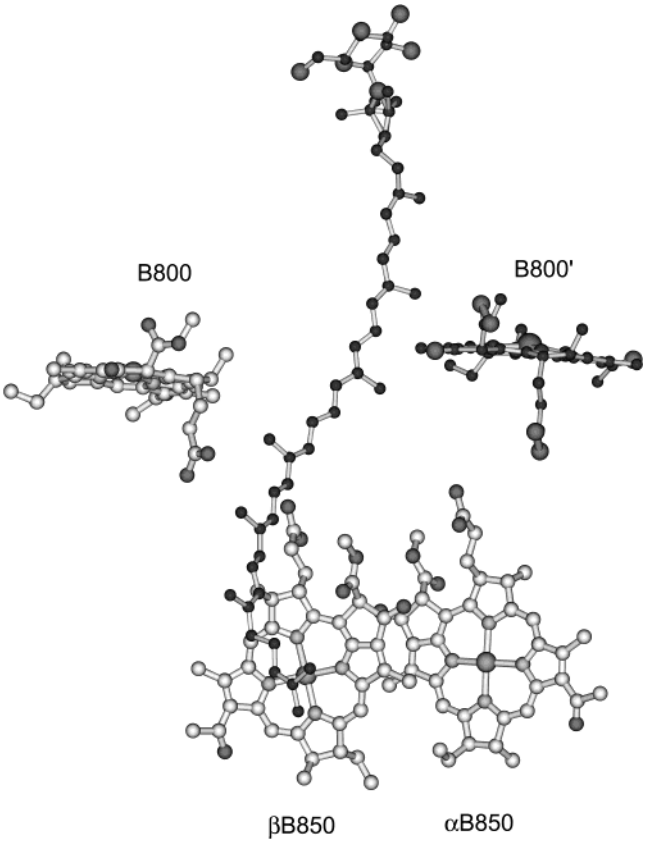

Figure 1. Arrangement of chromophores within the elementary building block of the LH2 complex (structural data taken from *Rps. acidophila* complex). The strongly coupled BChl*a* molecules absorbing at 850 nm are denoted αB850 and βB850 according to the binding protein subunit. The carotenoid molecule is located between the B850 and B800 BChl*a* molecules within the elementary unit. The B800 BChl*a* corresponding to the neighboring elementary unit is denoted B800′.

significant spectral overlap between the S_1 fluorescence and the absorption of the BChl molecules. These carotenoids can transfer energy via their S_1 state as revealed by a significant shortening of the carotenoid S_1 lifetime in the light-harvesting complex[9,12] compared with that observed in solution. This idea has also been supported by calculations.[17] In addition, the S_2-S_1 energy gap increases with conjugation length. The S_2 lifetimes of short carotenoids are on the order of less than 100 fs in solution.[35] On the bases of these results it was shown that the efficiency of S_1-mediated energy transfer decreases with increasing carotenoid conjugation length, dropping from 94% in a neurosporene (conjugation length of 9) containing LH2 complex from *Rb. sphaeroides*, to ∼80% for wild type *Rb. sphaeroides* LH2 (containing spheroidene, conjugation length of 10),[9] to only 5% in LH2 complexes from *Rps. acidophila* (containing RG, conjugation length of 11).[8] The efficiency of the S_2-mediated energy transfer in these complexes does not appear to change significantly with carotenoid conjugation length reaching typical values of 40−60%.[8,9,36] Thus, the S_1 route is critical for the overall efficiency of carotenoid-BChl energy transfer. LH2 complexes from *Rb. sphaeroides* exhibit 95% efficiency of the total carotenoid-BChl energy transfer. This decreases to 35−70% in the case of *Rps. acidophila*,[8,27] and falls as low as 30% for the LH1 complex from *Rhodospirillum rubrum* containing the carotenoid, spirilloxanthin, which has a conjugation length of 13.[37]

In this work, near-infrared femtosecond spectroscopy is used to determine the S_1 energies of spheroidene and RG in LH2 complexes. The data are important for understanding the energy

transfer pathways and mechanisms operating in these complexes. In addition, it is shown that relaxation processes in the LH2 complex of *Rb. sphaeroides* lead to the formation of a different transient carotenoid state, most likely a short-lived radical species, signaling the participation of charge-transfer states in the process of energy transfer between carotenoids and BChl*a* molecules.

2. Materials and Methods

The isolated LH2 complexes of both *Rb. sphaeroides* and *Rps. acidophila* were prepared according to ref 38. Spheroidene was extracted from whole cells of *Rb. sphaeroides* as described in ref 25. RG was prepared from LH2 from *Rps. acidophila* strain 10050 where it is the only carotenoid present. The LH2 sample was extracted in dichloromethane. The BChl was removed by portioning against 95% methanol/5% water. The carotenoid extract was dried down under nitrogen and resuspended in 40/60 BP petroleum ether. Pure RG precipitated from this final solution upon concentration by evaporation under nitrogen. All steps were carried out in a dark room. Prior to the experiments, all the samples were stored in the dark at −55 °C.

Measurements of carotenoids in solution were performed in *n*-hexane for spheroidene, and methanol for RG. Both solvents were of spectroscopic grade (Merck). The purified LH2 complexes were dissolved in a buffer (50 mM Tris, pH 8, 0.1% LDAO) having H_2O replaced by D_2O to allow measurements above 1300 nm where H_2O has strong absorption. It was verified that this change did not have any effect on the absorption spectra of the LH2 complexes. The optical density of all samples was ∼0.3 at the maximum of the 0−0 band of the carotenoid S_0-S_2 transition. All measurements were carried out at room temperature with the sample in a 2 mm path length quartz rotating cuvette, which avoided degradation. For the purified carotenoid solutions, a standard 2 mm spectroscopic glass cuvette was used.

The femtosecond spectrometer used in these studies is based on an amplified Ti:sapphire laser system (Spectra Physics), with tunable pulses obtained from two optical parametric amplifiers (Light Conversion) and/or white-light continuum generation. The femtosecond pulses emerging from the Ti:sapphire oscillator operating at a repetition rate of 82 MHz were amplified by a regenerative Ti:sapphire amplifier pumped by a Nd:YLF laser with a repetition rate of 5 kHz and producing ∼120 fs pulses with an average output power of ∼1 W at a central wavelength of 800 nm. For measurements in the near-infrared region, the amplifier output was divided by a 70/30 beam splitter to pump two independent parametric amplifiers for generation of the pump and probe pulses. The parametric amplifier used for generation of probe pulses was controlled by a computer, enabling direct scanning of the wavelength of the probe pulses over the spectral region 850−1800 nm. For measurements in the visible spectral region, white-light continuum pulses generated by focusing a fraction of the amplified light into a 5 mm sapphire plate were used for probing. In all experiments, the mutual polarization of the pump and probe beams was set to the magic angle (54.7°). The instrument response function was measured by generating sum frequency of the pump and probe pulses in a $LiIO_3$ crystal. The cross-correlation was fitted to a Gaussian function with a fwhm of 170−200 fs for measurements with the two optical parametric amplifiers (the actual fwhm depends slightly on the wavelength of the probing pulses) or 120−140 fs when the white-light continuum was used for probing. The excitation pulses were attenuated using neutral density filters to typical energies of 20−40 nJ/pulse. Steady-state absorption spectra were measured before and after the transient absorption experiments to ensure that no permanent photochemical changes had occurred.

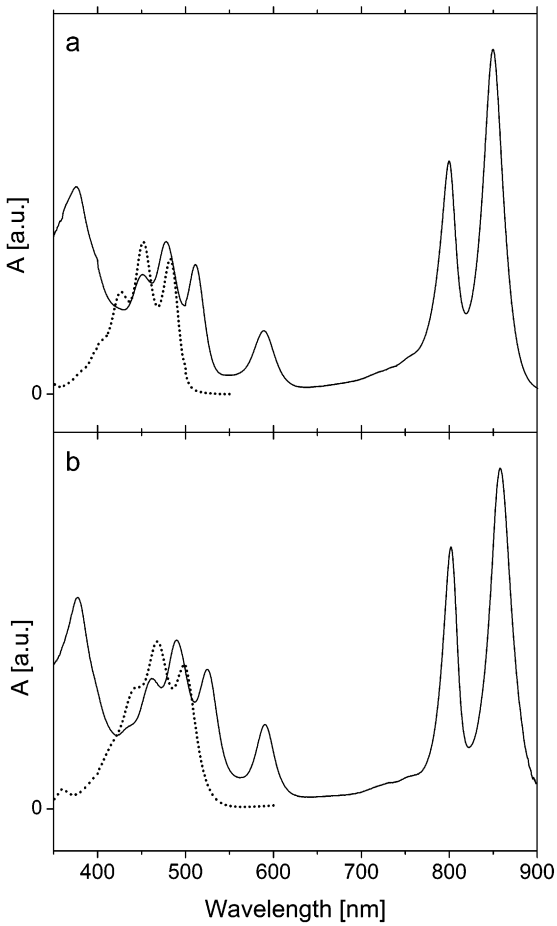

Figure 2. Steady-state absorption spectra of LH2 complexes (solid lines) from *Rb. sphaeroides* (a) and *Rps. acidophila* (b), together with absorption spectra of both carotenoids in solution (dashed lines): spheroidene in *n*-hexane (a) and RG in methanol (b).

3. Results

Absorption spectra of the LH2 complexes of *Rb. sphaeroides* and *Rps. acidophila* together with absorption spectra of the corresponding carotenoids in solution are shown in Figure 2. The LH2 absorption spectra exhibit characteristic spectral features in the near-infrared region due to B800 and B850 BChl*a* bands.[30] A distinct band located at around 590 nm in both LH2 species is the Q_x band of both B800 and B850 BChl*a* molecules. Below 550 nm, the vibronic peaks due to the S_0-S_2 transition of the carotenoids are observed. The 0−0 band of this transition is located at 512 nm (19530 cm^{-1}) for LH2 from *Rb. sphaeroides* containing the carotenoid spheroidene, which has 10 conjugated C═C bonds. The 0−0 band in *Rps. acidophila* is observed at lower energy peaking at 525 nm (19050 cm^{-1}) because RG has a conjugation length of 11. The energy gap between the vibrational bands of the S_0-S_2 transition is ∼1300 cm^{-1} resulting from a mixture of C−C (∼1100 cm^{-1}) and C═C (∼1500 cm^{-1}) stretching modes of the carotenoids. The same pattern is found in the absorption spectra of the carotenoids in solution, although a slightly larger energy difference between the 0−0 origins of the S_0-S_2 transitions of the two carotenoids, ∼700 cm^{-1} compared to ∼500 cm^{-1} for the molecules bound in the complexes, is observed. Moreover, the S_0-S_2 transitions

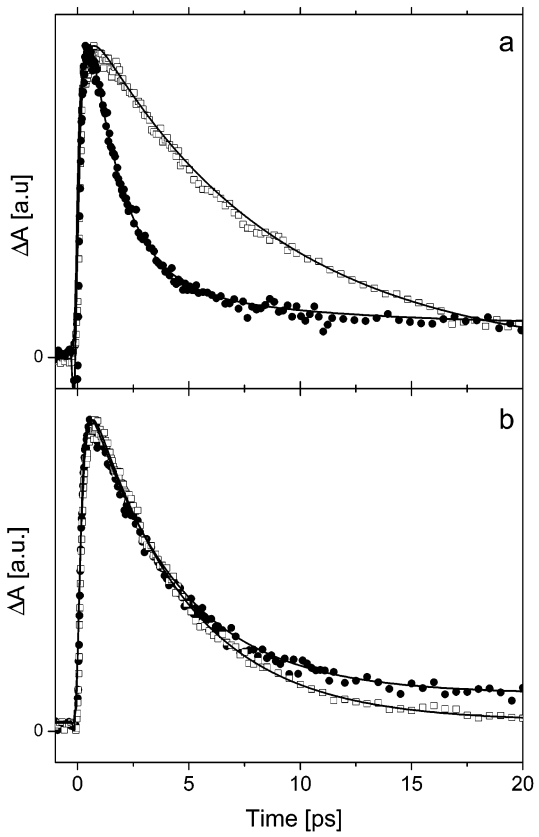

Figure 3. Kinetics recorded at the maximum of the S_1-S_N transition after excitation of the 0−0 band of the S_0-S_2 transition of the carotenoids. The S_1 decays of the carotenoids in solution (open symbols) and in the LH2 complex (full symbols) are compared for the LH2 complexes from *Rb. sphaeroides* (a) and *Rps. acidophila* (b). The corresponding fits of the kinetics are represented by solid lines. Excitation wavelengths are 515 nm (*Rb. sphaeroides*) and 525 nm (*Rps. acidophila*).

of both carotenoids in LH2 are shifted to lower energies by about 1000 cm^{-1} due to the interaction with the protein environment. The Soret band of BChl*a* is well-separated from the carotenoid bands peaking at around 380 nm in both LH2 complexes.

To obtain information about the S_1 state dynamics, the S_1 lifetimes of the carotenoids in the LH2 complexes and in solution were measured using the S_1-S_N transition occurring in the visible spectral region.[9,34] The kinetics measured at the peak of the S_1-S_N transitions are displayed in Figure 3. In the case of spheroidene, a dramatic change of the S_1 lifetime between LH2 and solution is observed. In solution the S_1 state decays monoexponentially with a time constant of 8.5 ps. In the LH2 complex, a significant shortening to 1.7 ps is observed. Also, a minor 8 ps component with amplitude of 10% is necessary to fit the kinetics recorded for LH2 complex. For RG in the *Rps. acidophila* LH2 complex, no significant change in the S_1 lifetime was observed compared to RG in solution. The fitting procedure yielded the S_1 lifetimes of 4.2 ps for RG in solution and 4 ps in LH2. It is also important to note that the S_1-S_N decay kinetics measured in both LH2 complexes required a low-amplitude nanosecond component to account for weak ESA of BChl*a* molecules in this spectral region (see Table 1).

Knowing the S_1 lifetime of both carotenoids in LH2, the near-infrared transient absorption spectra were measured at 2 ps after excitation. At this delay, the S_1 states of both carotenoids are still at least partially populated allowing detection of the carotenoid S_1 ESA. The near-infrared transient absorption

TABLE 1: Amplitudes of Time Constants Extracted from Multiexponential Global Fitting of Kinetics Measured at Various Probing Wavelengths for LH2 Complexes of *Rb. sphaeroides* (Excitation at 515 nm) and *Rps. acidophila* (525 nm)[a]

Rb. sphaeroides

λ[nm]	E [cm^{-1}]	τ_1 <0.2 ps	τ_2 1.7 ± 0.4 ps	τ_3 8 ± 0.7 ps	τ_4 ~1 ns
560	17850	−100	84	10	6
970	10300	83		16	1
1080	9260	91	1.5	2.5	5
1200	8330	91	−1	0.5	9
1400	7140	67	6	9	18
1500	6660	64	14.5	4.5	17
1600	6250	14	38	2	46
1700	5880	2	48	1	49

Rps. acidophila

λ [nm]	E [cm^{-1}]	τ_1 <0.2 ps	τ_2 0.8 ± 0.1 ps	τ_3 4 ± 0.4 ps	τ_4 ~1 ns
580	17240	−100		92	8
970	10300	87	4	8.5	0.5
1080	9260	83.5	8	2.5	6
1200	8330	94	0.5	1.5	4
1400	7140	74	7	8	11
1500	6660	-	32	37	31
1600	6250	60	11	11	18
1700	5880	39	21.5	1.5	38

[a] Time constants τ_1 and τ_4 were fixed during the fitting procedure, while the τ_2 and τ_3 were used as fitting parameters. Results of global fitting were verified by fitting kinetics individually, confirming that the results of individual and global fitting do not differ by more than 10%.

spectra recorded 2 and 20 ps after excitation into the 0−0 vibrational band of the S_0-S_2 transition at 515 nm for *Rb. sphaeroides* and 525 nm for *Rps. acidophila* are shown in Figure 4. Since the carotenoid ESA in the near-infrared region is much weaker than that corresponding to the S_1-S_N transition in visible region, the relative contribution from the BChl*a* ESA will be much stronger in the infrared. To allow an unequivocal assignment of the BChl*a* ESA, the transient absorption spectra after excitation of the B850 BChl*a* band are shown for comparison.

The most striking difference between the transient absorption spectra of the two LH2 complexes is at the high-energy side of the near-infrared region. Although the transient absorption spectrum of LH2 from *Rps. acidophila* is rather featureless below 1400 nm at all delay times, the transient spectrum of LH2 from *Rb. sphaeroides* measured at 2 ps delay is dominated by a strong ESA band centered at 960 nm (10415 cm^{-1}). At longer delay times, this band disappears and the transient absorption spectra of both LH2 complexes become quite similar. The origin of the 960 nm band, which is clearly due to spheroidene since it is not observed when B850 is excited directly, will be described in detail in the Discussion section.

The transient absorption spectra of both carotenoids exhibit a similar feature located at around 1610 nm (6200 cm^{-1}) for *Rb. sphaeroides*, and at 1540 nm (6500 cm^{-1}) for *Rps. acidophila*. Because this band is not observed either when the B850 band is excited directly or 20 ps after carotenoid excitation, it is assigned to the S_1-S_2 transition of carotenoids. In case of spheroidene, the second vibrational band of this transition is observed at around 1360 nm (7350 cm^{-1}). The higher vibrational bands of this transition, which are clearly visible for carotenoids in solution,[24,25] are obscured by the BChl*a* ESA band located between 1100 and 1300 nm for LH2 from both species. To confirm the assignment of the low-energy bands to the caro-

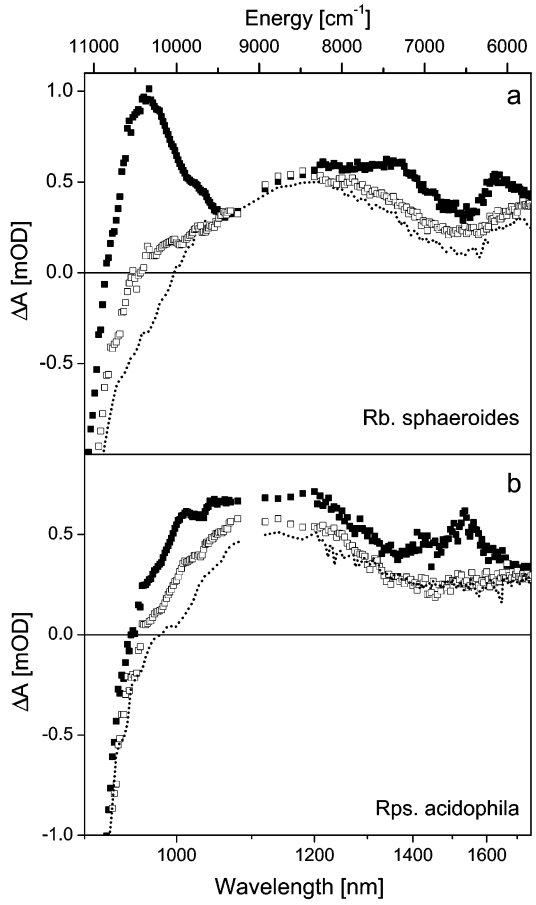

Figure 4. Near-infrared transient absorption spectra of LH2 complexes from *Rb. sphaeroides* (a) and *Rps. acidophila* (b) recorded at 2 ps (full squares) and 20 ps (open squares). Excitation wavelengths are 515 nm (*Rb. sphaeroides*) and 525 nm (*Rps. acidophila*). The transient absorption spectrum measured after excitation of the B850 band is shown for comparison (dotted line). The B850 band was excited at 850 nm for both complexes. The transient spectrum after 850 nm excitation was normalized to have the same magnitude of B850 bleaching as the transient spectra excited in the carotenoid region.

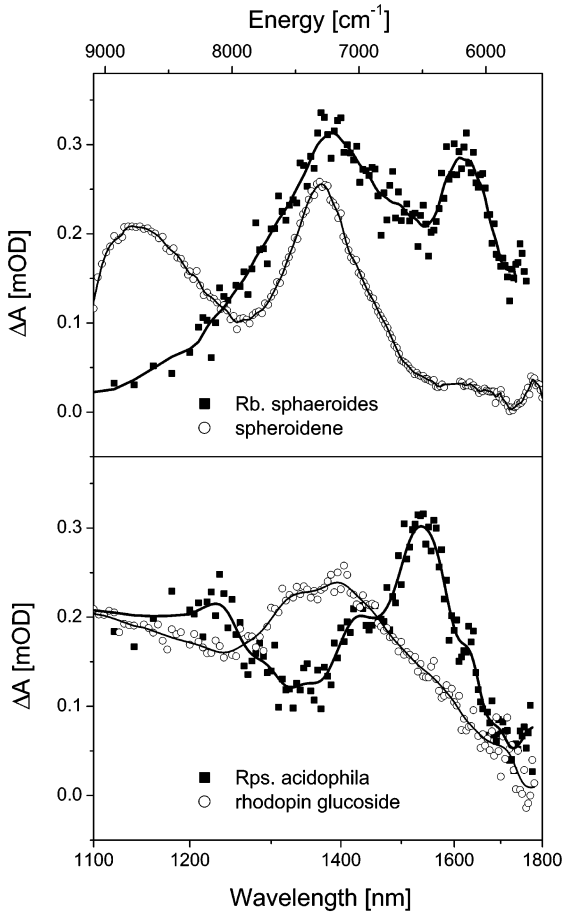

Figure 5. Differential transient absorption spectra after subtraction of the BChl*a* signal of the LH2 complexes from both LH2 species (full squares), together with the S_1-S_2 profiles of the corresponding carotenoids in solution (open circles). The solid lines represent FFT-filter smoothing of the data.

tenoid S_1-S_2 transition, the differential transient absorption spectra (DTAS) in the spectral range 1100−1800 nm obtained by subtraction of the B850 ESA are compared with near-infrared transient absorption spectra of the corresponding carotenoids in solution (Figure 5). The overall shape of the transient absorption spectrum of spheroidene in solution is similar to the DTAS of spheroidene in LH2, although the DTAS of spheroidene in LH2 is shifted by 1150 cm^{-1} to lower energy as a result of a decrease of the S_1-S_2 energy gap due to interaction with the protein. In the case of *Rps. acidophila*, both the transient absorption spectrum of RG and the DTAS of RG in LH2 complex exhibit similar features as those of spheroidene. For RG, however, the lowest energy band of the transient absorption spectrum of RG in solution centered at ∼1390 nm (7200 cm^{-1}) is broader than that observed in the DTAS spectrum of RG in LH2. The redshift of the DTAS of RG in LH2 is ∼700 cm^{-1}, which is smaller than that observed for spheroidene (∼1100 cm^{-1}).

To reveal the origin of the spectral features in the transient absorption spectra, we measured kinetics at various wavelengths spanning the 900−1800 nm spectral region for both LH2 complexes. The kinetics measured at wavelengths corresponding to the spectral bands observed in the transient absorption spectrum are shown in Figure 6. For *Rb. sphaeroides*, all the kinetics could be fitted globally with four time constants of <200 fs, 1.7 ps, 8 ps and 1 ns, demonstrating that the decay components obtained from the fitting of the S_1-S_N decay (Figure 3) are sufficient to fit kinetics at all other wavelengths. The shortest subpicosecond process dominates at higher energies, while in the kinetics measured at lower energy this component is almost negligible. Notably, the 1.7 ps component, which is the spheroidene S_1 lifetime in the LH2 complex, is the main decay component of the kinetics measured at 1600 nm, but it has a very low amplitude in the kinetics recorded at the maximum of the 960 nm band. Exactly the opposite situation occurs for the 8 ps component. This process dominates the kinetics probed at 960 nm, but the amplitude of this component drops to 2% when kinetics are recorded at 1600 nm. This is a clear indication that the 1600 and 960 nm bands in the transient absorption spectrum of the LH2 complex from *Rb. sphaeroides* occur from different processes. The kinetics measured at 1400 nm (see Table 1) contains both 1.7 and 8 ps components with about the same amplitudes. In all kinetics the 1 ns component is necessary to take into account the ESA of B850 BChl*a* molecules. To examine the spectral variation of the amplitudes of the 1.7 and 8 ps components, kinetic traces measured at 15 different wavelengths were fitted globally and real amplitudes of these two components were plotted as a function of probing wavelength. The spectral profiles of the amplitudes of 1.7 and 8 ps components are shown in Figure 7. The 1.7 ps component has a clear maximum at around 1600 nm suggesting its connection with a decay of the S_1-S_2 transition. It is worth noting that, at 1200 nm, the 1.7 ps component has a weak

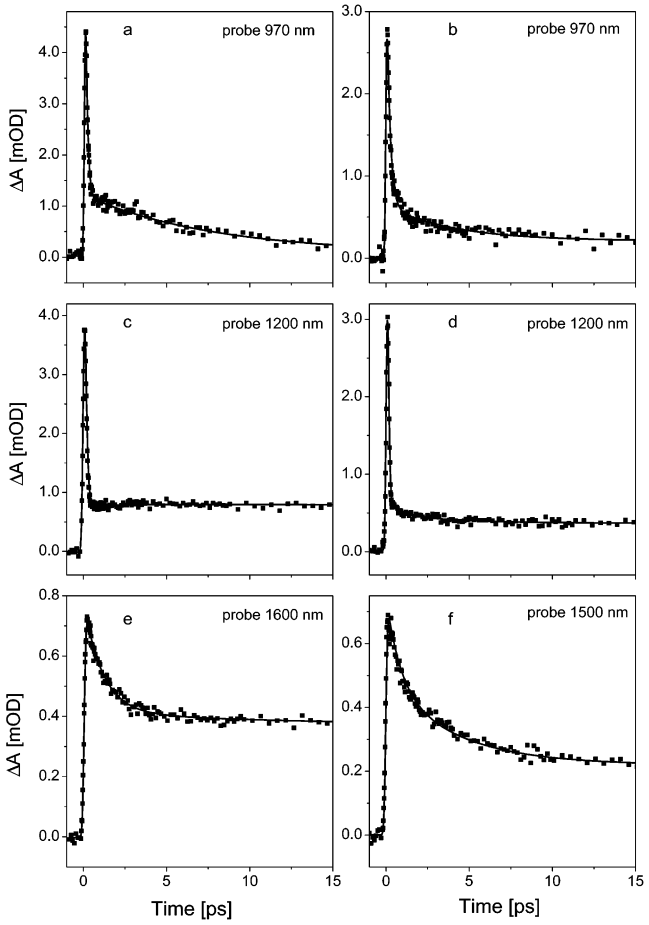

Figure 6. Kinetics recorded in the infrared region after excitation of the carotenoids in the LH2 complexes from *Rb. sphaeroides* (left column, excitation at 515 nm) and *Rps. acidophila* (right column, excitation at 525 nm). The selected probing wavelengths correspond to the maximum of the 960 nm band (a,b), to the maximum of BChl*a* ESA (c,d), and to the 0−0 band of the S_1-S_2 transition (e,f). Corresponding fits of the kinetics are represented by solid lines.

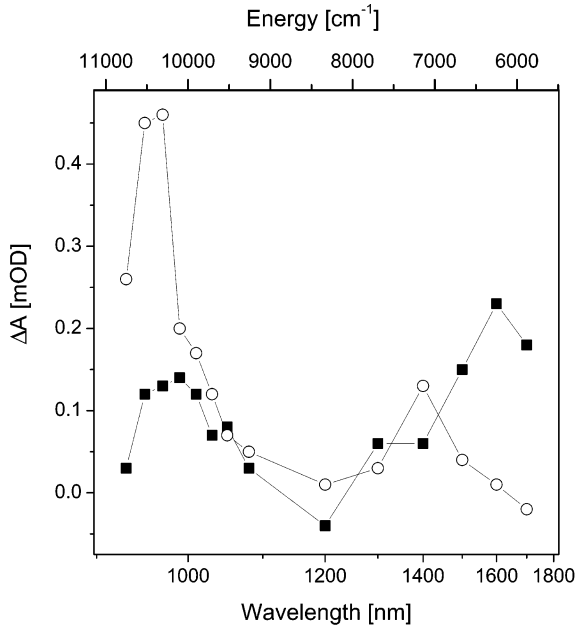

Figure 7. Spectral profiles of the amplitudes of the 1.7 ps (full squares) and 8 ps (open circles) components as extracted from multiexponential global fitting of the kinetics recorded for the LH2 complex from *Rb. sphaeroides* after excitation of spheroidene at 515 nm.

negative amplitude showing that it is a rise component in the kinetics recorded at 1200 nm (see also Figure 6c). This result confirms that BChl*a* ESA dominates at this wavelength and the 1.7 ps component represents energy transfer from spheroidene to BChl*a*. Contrary to the 1.7 ps time component, a process characterized by a 8 ps time constant has a distinct maximum at around 960 nm, with a weaker, but pronounced band at around 1400 nm.

For *Rps. acidophila*, the situation is more complicated because it is not possible to obtain reliable fits using only the decay components extracted from the fitting of the S_1-S_N ESA. It is apparent from global fitting that one more subpicosecond component with a time constant of 0.8 ps is required in addition to the <200 fs, 4 ps, and 1 ns components. Then, the spectral profile of the <200 fs component is similar to that observed for *Rb. sphaeroides*, as it is much stronger on the high-energy side. The 0.8 and 4 ps components are included in all kinetics with comparable amplitudes, although they are almost negligible in the kinetic recorded at 1200 nm, because, as one can see from the transient absorption spectrum, at this wavelength almost all of the signal after the initial 0.2 ps relaxation comes from B850 having a 1 ns lifetime. The results of multiexponential global fitting of kinetics recorded at various probing wavelengths for both LH2 complexes are summarized in Table 1.

4. Discussion

The difference between the pattern of energy transfer pathways in the two studied LH2 complexes is clear from the kinetics measured at the maximum of the S_1-S_N transition shown in Figure 3. The shortening of the spheroidene S_1 lifetime in the LH2 complex (1.7 ps) as compared with solution (8.5 ps) indicates an S_1-mediated energy transfer efficiency of about 80% in the LH2 complex from *Rb. sphaeroides*, in good agreement with previous studies.[9,12,27] On the other hand, almost no change of the RG S_1 lifetime was observed when measured in methanol compared to that in the LH2 complex, suggesting that the RG molecule in the LH2 complex of *Rps. acidophila* is not utilizing this energy transfer pathway to any significant extent. The alternate S_2 pathway is apparently used in both LH2 complexes as shown by comparison of the carotenoid S_2 lifetimes in the LH2 complexes and in solution. The efficiency is slightly lower in *Rb. sphaeroides* yielding a value of ∼40%[36] compared to that of *Rps. acidophila*, in which a value of 51% was reported.[8] It is worth noting, however, that the actual values of the S_2 energy transfer efficiency may be systematically in error, since the carotenoid S_2 lifetimes decrease with increasing refractive index of the medium. Thus, they are not the same for various solvents, as addressed by Macpherson et al.[8] This problem is avoided in the case of S_1 energy transfer, because no solvent dependence of the S_1 lifetime was observed for carotenoids without carbonyl groups.[39]

To rationalize the dramatic difference between the efficiency of the S_1 energy transfer pathway in the two LH2 complexes, we determine the S_1 energies of spheroidene and RG in LH2 complexes on the basis of the near-infrared transient absorption spectra shown in Figures 4 and 5. The spectral bands occurring in both LH2 species at the low-energy edge of the transient absorption spectrum located at 6200 cm^{-1} (*Rb. sphaeroides*) and at 6500 cm^{-1} (*Rps. acidophila*) are clearly due to the carotenoid S_1 ESA, because they are not observed in the transient spectrum after B850 excitation and they disappear within the lifetime of the carotenoid S_1 state. The energy and spectral width of these bands correspond well to the 0−0 band of the S_1-S_2 transition of xanthophylls in LHCII having the

conjugation length 9−11.[29] Because spheroidene and RG have conjugation lengths of 10 and 11, respectively, strong support is made for the assignment of the 6200 cm^{-1} (*Rb. sphaeroides*) and 6500 cm^{-1} (*Rps. acidophila*) bands in the transient absorption spectrum shown in Figure 4 to the 0−0 vibrational band of the S_1-S_2 transition of both carotenoids. A direct comparison of the transient absorption spectra of LH2 complexes and carotenoids in solution in the spectral region 1100−1800 nm (Figure 5) provides additional support to this assignment. Subtraction of the BChl*a* contribution clearly reveals the 0−1 vibrational band in the transient absorption spectrum in the LH2 complex from *Rb. sphaeroides*. The energy distance between the 0−0 and 0−1 vibrational bands corresponds well to the energy difference between vibrational bands of the carotenoid S_2 state, supporting our assignment of the spectral feature in the transient absorption spectrum to the spectral profile of the lowest vibrational band of the S_1-S_2 transition. In the case of *Rps. acidophila* the transient spectrum is shifted to higher energies and suffers significantly from overlap with the BChl*a* contribution, which precludes the observation of higher vibrational bands.

In general, the 0−0 bands of the carotenoid S_1-S_2 transition observed in the LH2 complex are shifted to lower energies compared with those of the carotenoids in solution. This is a consequence of a markedly different effect of the protein environment on the S_1 and S_2 energies leading to the observed contraction of the S_1-S_2 energy gap. A similar effect is also known to occur for the S_1-S_N transition and very recently, it was also observed for the S_1-S_2 transition of carotenoids in an LHCII complex.[29] A direct comparison of the widths of the 0−0 bands of both carotenoids in solution and in the LH2 complex also shows substantial changes. In the case of spheroidene the width of the 0−0 bands are about the same in solution and in the LH2 complex. For RG, however, the 0−0 band in the LH2 complex is markedly narrower than in solution. This result can be explained by the fact that in the LH2 complex only one particular conformation of the carotenoid is achieved, while a mixture of different conformations can coexist in the S_1 state for a carotenoid in solution as discussed in ref 25. Limiting the carotenoid conformation would lead to the observed narrowing of the vibrational bands of the S_1-S_2 transition. This effect is stronger for RG, most likely due to the presence of the glucoside ring introducing a strong asymmetry in the carotenoid molecule that facilitates the formation of conformers in the S_1 state. This effect is noticeable even for the S_2 state as one can see from Figure 2: the RG absorption spectrum exhibits a more pronounced structure of vibrational bands in the LH2 complex than in solution, which is a clear sign of less conformational disorder in LH2 complex.

The results of a global fitting procedure summarized in Table 1 show that in the case of *Rb. sphaeroides*, the kinetics measured at 550 nm (corresponding to the S_1-S_N transition) is in perfect match with those recorded at 1600 nm, supporting our assignment of the bands. The changes in amplitudes of the decay components are caused by much stronger relative contribution from the BChl*a* ESA in the infrared region. The S_1-S_N kinetic trace for RG in the LH2 complex of *Rps. acidophila*, however, exhibits a deviation from that measured at 1500 nm. The kinetics recorded in the infrared region contain an additional 0.8 ps component, which is clearly not necessary to fit the kinetics recorded at 550 nm. This difference can be explained by the S_2 energy transfer pathway operating in the LH2 complex from *Rps. acidophila*. It was shown that the energy transferred from the S_2 state of RG is accepted by the Q_x states of both B800 and B850 with a similar efficiency.[8] Therefore, the subpicosecond component observed in the 1500 nm kinetics is most likely due to a decay of the B800 ESA reflecting B800−B850 energy transfer. The dynamics of this process are well documented[30] and the 0.8 ps component observed here matches well the dynamics of the B800 to B850 energy transfer in LH2 of *Rps. acidophila*. Also, the fact that the 0.8 ps component becomes dominant at 1700 nm (see Table 1) supports the conclusion that it is not due to the RG dynamics, because this wavelength is at the very edge of the S_1-S_2 transition (Figure 5). This result has an interesting consequence in terms of different energy transfer pathways in *Rb. sphaeroides* and *Rps. acidophila*. Since no component corresponding to the B800−B850 energy transfer was observed in the infrared region in the LH2 complex from *Rb. sphaeroides*, it suggests that the S_2−B800 Q_x pathway is negligible in this species, contrary to *Rps. acidophila*, where the S_2−B800 Q_x and S_2−B850 Q_x energy transfer channels operate with about the same efficiency.[8] In fact, the kinetics recorded in B800 region after excitation of the carotenoid in LH2 of *Rb. sphaeroides*[12,40] show only a weak B800 bleaching at early times, providing additional support to this conclusion. Thus, although the kinetics measured at the maximum of the S_1-S_2 transition has an additional component due to B800−B850 energy transfer in the case of LH2 from *Rps. acidophila*, we can conclude that the infrared transient spectrum measured at 2 ps delay shown in Figures 4 and 5 indeed reflects the spectral profile of the S_1-S_2 transition of RG, since most of the signal at 2 ps originates from the carotenoid.

Having assigned the bands in the infrared transient absorption spectra, we can calculate the S_1 energy of both carotenoids in LH2 complexes by subtracting the 0−0 energies of the S_0-S_2 and S_1-S_2 transitions. This procedure yields the S_1 energies of 13400 ± 100 cm^{-1} (spheroidene) and 12550 ± 150 cm^{-1} (RG). The energy of 12550 ± 150 cm^{-1} for RG in LH2 agrees with the results of time-dependent density functional theory (TDDFT) calculations,[17] where the upper bound of 13000 cm^{-1} was inferred for the S_1 energy of RG in LH2. It is interesting to compare these values with those obtained for both carotenoids in solution. The S_1 energy of spheroidene in *n*-hexane was determined to be 13400 cm^{-1} by means of femtosecond spectroscopy,[25] thus exactly the same as in the LH2 complex. The S_1 energy of RG in methanol solution was calculated from the 0−0 energies of the S_0-S_2 and S_1-S_2 transitions shown in Figures 2 and 5, yielding a value of 12800 ± 200 cm^{-1}. Thus, in the case of *Rps. acidophila*, the S_1 state in LH2 complex is slightly red-shifted as compared with that measured in methanol solution, but this discrepancy can be due to the rather broad S_1-S_2 profile of RG in solution. As noted above, this broadness is most likely a result of a mixture of various conformers occurring in solution, thus, it is not straightforward to compare the S_1 energy in solution with the energy measured in the LH2 complex, since in the LH2 complex only one particular conformation of RG is likely present.

Thus, using the S_1 energies of both carotenoids in the LH2 complex, the different energy transfer pathways in *Rb. sphaeroides* and *Rps. acidophila* can be rationalized. As shown recently by calculations,[17] the S_1 energy transfer rate in the LH2 complex is fast and rather insensitive to the position of the S_1 state in the energy range of 13500−15000 cm^{-1}, while for energies below 13000 cm^{-1} the S_1 energy transfer pathway becomes inefficient yielding carotenoid S_1 to BChl energy transfer rates lower than $(30\ ps)^{-1}$. The result of the TDDFT theory is in good agreement with the S_1 energies obtained here. The S_1

energy 13400 cm^{-1} of spheroidene in LH2 is at the edge of the high-efficiency interval, which results in effective energy transfer from the S_1 state of spheroidene to BChls. In LH2 of *Rps. acidophila*, however, the S_1 energy of RG (12550 cm^{-1}) is shifted out of this interval and the S_1-Q_y pathway becomes negligible, as demonstrated by the same S_1 lifetime of RG in solution and in the LH2 complex.

Although the low-energy edge of the near-infrared transient spectra gives important information about the S_1 energies of both carotenoids, the most striking difference between the LH2 complexes of the two different bacteria is the 960 nm band in the transient absorption spectrum of *Rb. sphaeroides* recorded at 2 ps. From previous measurements on spheroidene in solution it is known that the ESA signal corresponding to the higher vibrational bands of the S_1-S_2 transition is weak below 1000 nm,[25] suggesting that the 960 nm band is most likely of a different origin. Furthermore, the energy gap between the 960 nm band and the 0−0 band of the S_1-S_2 transition indicates that the 960 nm band cannot be a part of the vibrational progression of the S_1-S_2 transition. In addition, the 960 nm band decays almost exclusively with an 8 ps time constant, leading to the conclusion that its origin is not due to the S_1-S_2 transition. On the other hand, since B850 excitation (Figure 4) does not produce any ESA in this spectral region and the 8 ps lifetime of the 960 nm band is too long to be assigned to ESA of B800 BChl*a* molecules, the origin of the 960 nm band must be due to spheroidene. Since the 8 ps decay matches well the S_1 lifetime of spheroidene in solution and the low amplitude (∼10%) 8 ps decay component was also observed in the S_1-S_N spectral region (see Figure 3 and Table 1), it may be tempting to assign this species to spheroidene molecules that do not transfer energy to BChls. However, as noted above, the near-infrared S_1-S_2 transient absorption spectrum of spheroidene in solution does not contain any distinct band between 900 and 1000 nm and thus this possibility can be excluded.

The spectral profiles of the decay components shown in Figure 7 are the key data to reveal the origin of the 960 nm band. The spectral profile of the 8 ps component remarkably resembles the absorption spectrum of a carotenoid radical cation, which exhibits a distinct absorption band located between 900 and 1000 nm with an extinction coefficient comparable to that of the S_0-S_2 transition,[41] which is due to the D_0-D_2 transition according to the notation for electronic states of polyene radical cations.[42] A weaker, D_0-D_1 transition is located in the near-infrared region peaking between 1200 and 1400 nm,[41] which is again in good agreement with the spectral profile of the 8 ps component exhibiting a weaker, but pronounced, band around 1400 nm. To support this assignment further, we measured the spectrum of the spheroidene radical in methanol solution using UV excitation,[43] since it is known that the UV flash photolysis can produce long-lived carotenoid radicals.[44,45] A comparison of the spheroidene radical absorption spectrum with the 960 nm band observed in the LH2 transient absorption spectrum is presented in Figure 8. The spectrum in solution has a maximum at 905 nm, shifted by about 650 cm^{-1} to higher energy from the maximum of the 960 nm band, but the overall shape of both spectral features is quite similar. In fact, the ∼650 cm^{-1} shift of the 960 nm band toward lower energies in LH2 can be explained by the interaction with the protein environment, because the magnitude of the shift is almost identical with that observed for the β-carotene radical in the Photosystem II reaction center compared with the solution.[41,46] The narrower 960 nm band compared with the methanol solution is caused by interference with the B850 bleaching, which affects the high-energy part of the 960 nm band.

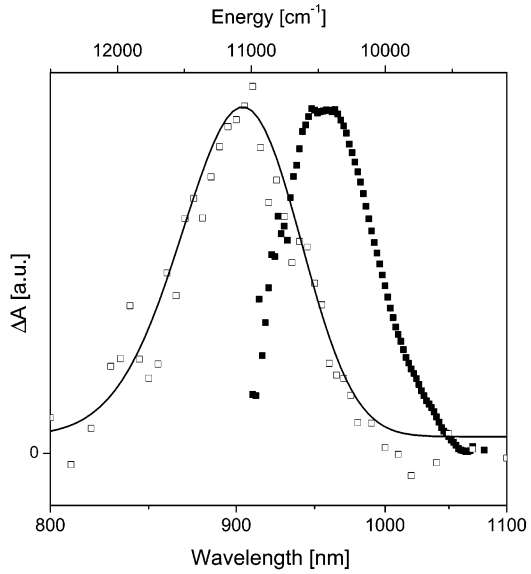

Figure 8. Comparison of the differential transient absorption spectrum of the LH2 complex of *Rb. sphaeroides* (BChl*a* ESA subtracted) in the region 900−1100 nm obtained after excitation of spheroidene at 515 nm (full squares), with the spectrum of the spheroidene radical generated in methanol solution (open squares).[43] The solid line represents a Gaussian fit of the radical spectrum. Both spectra are normalized to the maximum.

The position and shape of the 960 nm band supports our assignment of this band to the spheroidene radical cation formed transiently in the LH2 complex. The lifetime of 8 ps, which is much shorter than the known radical lifetimes in the millisecond time scale,[47] suggests a rather unusual behavior of spheroidene in the LH2 complex. Also, the ultrafast (<200 fs) formation of this species is not typical for radicals, although it was shown recently for β-carotene in chloroform that a radical cation can be indeed formed within 140 fs directly from the originally excited S_2 state.[48]

The discussion above highlights the intriguing spectral characteristics of the 8 ps decay component observed in the LH2 complex from *Rb. sphaeroides*. On one hand, it has spectral properties reminiscent of a spheroidene cation radical (the 960 nm band), but it has also spectral components in the visible spectral region that cannot be assigned to the spheroidene radical and that coincide with the S_1-S_N ESA of spheroidene. On the other hand, the 8 ps component observed in the visible spectral region cannot be assigned to the S_1-S_N transition, because that would lead to a 8 ps decay component present also in the S_1-S_2 ESA, contrary to the observations. Thus, we conclude that the 8 ps decay components in the near-infrared and visible spectral regions are of different origins. We have already shown that the near-infrared species (the 960 nm band) may be attributed to a radical species, but the origin of the 8 ps component observed in the visible spectral region is less clear. It is obviously not related to spheroidene molecules decoupled from energy transfer to BChls, but it could perhaps be due to the newly identified S* state found in the LH1 complex of *Rs. rubrum*.[7] Very recently, it was confirmed that this state is present also in the LH2 complex of *Rb. sphaeroides* and has a lifetime of 7 ps.[49] The relation between the radical formation and population of the S* state is not known and will be certainly a subject of further studies. It is also necessary to note that, similarly to the yield of the S* state formation in *Rb. sphaeroides*,[49] the yield of the spheroidene radical in LH2 is rather low.

TABLE 2: Ten First Low-Lying Excited States of the Carotenoid-B800′ Complex from B3LYP/6-31G* Calculations[a]

state	energy (cm^{-1})	oscillator strength	main configuration and the corresponding amplitude for CT states
CT	3100	0.0	0.705 HOMO (Car) → LUMO (B800′)
CT	9100	0.0004	0.703 HOMO-1 (Car) → LUMO (B800′)
CT	14380	0.0229	0.691 HOMO-2 (Car) → LUMO (B800′)
Q_y (B800′)	14630	0.6595	
CT	15360	0.0012	0.703 HOMO (Car) → LUMO + 1 (B800′)
CT	17170	0.0040	0.693 HOMO-2 (Car) → LUMO + 2 (B800′)
Q_x (B800′)	18730	0.0398	
	19300	0.0	no clear assignment possible
S_1 (Car)	19615	0.1246	
S_2 (Car)	16680	3.6729	

[a] Orbital assignment to carotenoid or B800′ is based on visual inspection.

The intensity of the 960 nm band is about 50 times weaker than the intensity of the B850 bleaching signal (data not shown). Taking into account that the extinction coefficient of the D_0-D_2 transition of carotenoid radical cations is about the same as that of the S_0-S_2 transition of neutral carotenoids,[41] and knowing the carotenoid-BChl energy transfer efficiencies, a rough estimate gives a yield of 5−8% of the spheroidene radical, suggesting that only a minor fraction of the initially excited spheroidene molecules will form the radical cation.

The exact mechanism of the spheroidene radical formation in LH2 cannot be directly inferred from the data presented here. Nevertheless, its ultrafast formation followed by a decay occurring on the picosecond time scale suggests that it is certainly not due to a diffusion limited process, but rather points to the fact that an electron acceptor is fixed in close proximity to spheroidene. In such a case the electron acceptor is likely one of the neighboring BChl molecules and short-lived charge stabilization is allowed due to protein environment. The fact that the radical formation is significantly more effective in the case of *Rb. sphaeroides* (although a weak signal in this region is also present in *Rps. acidophila*) would suggest slight structural differences in the vicinity of the carotenoid molecule for these two LH2 complexes.

To investigate the possible origin of the carotenoid radical we have performed computational studies for the low-lying excited states of the carotenoid-B800′ BChl complex (see Figure 1) using the crystal structure of *Rps. acidophila*.[31] The current resolution of the structure is not sufficient to position the hydrogen atoms and to provide the correct conjugated carbon−carbon bond lengths for the carotenoid. Hydrogen atoms were added and their positions were optimized at the Hartree−Fock (HF) level by using the 6-31G basis set. The conjugated carbon−carbon bond lengths of the carotenoid RG were optimized using density functional theory (DFT) based on the three-parameter Lee−Yang−Parr (B3LYP) functional[50] with 6−31G** basis set. In all calculations the Gaussian 98 program package was used.[51] The other nearby BChls are modeled via atomic point charges obtained from the RHF/6−31G* calculations to represent the local electrostatic field of LH2.[52] The first 10 excited states of the carotenoid-B800′ complex was calculated using the time-dependent DFT/B3LYP with 6-31G* basis set. Visual inspection of the orbitals that are involved in the main configurations of the excited states enabled us to identify the excited states corresponding to the transitions of the individual molecules: the Q_y-Q_x transitions of B800′ and the S_1-S_2 transitions of the RG. Besides these conventional transitions, a few excited states of the complex which involve the transitions from the occupied valence orbitals of the carotenoid to π^* orbital of B800′ was found in the region of the B800 Q-bands (see Table 2). These intermolecular charge-transfer (CT) states may become populated after fast relaxation from the initially excited carotenoid S_2 state. Such population of the CT states can be a precursor of a real charge separation leading to an ESA signal, which corresponds to the observed absorption of the radical cation. Thus, the calculations show that a scenario involving CT states of the carotenoid-BChl complex can explain the radical signal. It is necessary to point out, however, that there are certain limitations. First, due to the lack of knowledge of LH2 structure of *Rb. sphaeroides*, the calculations were performed only for *Rps. acidophila*, where the radical signal is much weaker than in *Rb. sphaeroides* and, consequently, quantitative information cannot be obtained. Second, the 6-31G* basis set used in our calculations is obviously not capable to obtain the right ordering of the S_1 and S_2 states of the carotenoid (see Table 2). Extending the basis set to 6-31++G** would solve the problem as can be seen from TDDFT calculations of carotenoids,[17] but for the carotenoid-BChl complex such calculations are beyond the limits of current computational capabilities. Thus, although the calculations show that CT states are indeed present in the excited-state manifold of the carotenoid-BChl complex in LH2, further experimental and theoretical work is needed to reveal their roles in the cation radical formation and energy transfer processes between carotenoids and BChls.

5. Conclusions

Probing both the visible and near-infrared spectral regions of LH2 complexes from two species of purple bacteria, *Rb. sphaeroides* and *Rps. acidophila*, by means of femtosecond transient absorption spectroscopy enabled the determination of important information about energetics and dynamics of carotenoids in these complexes. The results achieved within this study can be summarized as follows:

(1) By measurements in the near-infrared region after carotenoid excitation, the spectral profiles of the carotenoid S_1-S_2 transitions have been obtained, which enables a determination of the S_1 energies of the carotenoids in the LH2 complexes from both species. In the case of *Rb. sphaeroides*, the S_1 energy of the carotenoid spheroidene is 13400 ± 100 cm^{-1} (746 ± 5 nm). This value is high enough to allow efficient energy transfer from the spheroidene S_1 state to BChls. In *Rps. acidophila*, the S_1 energy of the carotenoid rhodopin glucoside, which has longer conjugation length than spheroidene, drops to 12550 ± 150 cm^{-1} (797 ± 9 nm). This lowering of the S_1 energy leads to a poor efficiency of the S_1 energy transfer channel in this species. In addition, by comparison with S_1-S_2 spectral profiles of both carotenoids in solution, we concluded that in the case of spheroidene it is feasible to approximate the S_1 energy in the LH2 complex by the value measured in solution, as no difference (within experimental error) between these values was observed. For RG, exhibiting a larger degree of spectral inhomogeneity in solution such approximation is not straightforward, because the S_1 energies of different conformers occurring in solution can differ from the S_1 energy of the particular conformation of the RG molecule in LH2.

(2) In the LH2 complex from *Rb. sphaeroides*, an additional band peaking at around 960 nm was observed in the transient absorption spectrum after excitation of spheroidene. This band, which was not observed when BChls are excited, exhibits different dynamics than spheroidene S_1 state. While the S_1 state decays with a 1.7 ps time constant indicating the efficient S_1 energy transfer pathway, the 960 nm band exhibits a decay characterized by an 8 ps lifetime. The spectral profile of this time component in the near-infrared spectral region sugests that the 960 nm band is due to ultrafast formation of a spheroidene radical cation in the LH2 complex, which then decays with a time constant of 8 ps. The yield of spheroidene radical formation is estimated to be in the range of 5−8%.

Acknowledgment. We thank James Bautista for technical assistance with the spheroidene sample and to Emmanouil Papagiannakis and Rienk van Grondelle for sharing their results (Ref. 49) prior to publication. The work at Lund University was performed with funding from the Swedish Research Council, the Wallenberg Foundation and the Crafoord Foundation. R.J.C. thanks the BBSRC for financial support. The work in the laboratory of H.A.F. has been supported by grants from the National Institute of Health (GM-30353) and the National Science Foundation (MCB-9816759).

References and Notes

(1) Ritz, T.; Damjanovic, A.; Schulten, K.; Zhang, J.-P.; Koyama, Y. *Photosynth. Res.* **2000**, *66*, 125.

(2) Frank H. A.; Cogdell R. J. *Photochem. Photobiol.* **1996**, *63*, 257.

(3) Edge, R.; McGarvey, D. J.; Truscott, T. G. *J. Photochem. Photobiol.* **1997**, *41*, 189.

(4) Christensen, R. L. In *Photochemistry of Carotenoids*; Frank, H. A., Young, A. J., Britton, G., Cogdell, R. J., Eds.; Kluwer Academic Publishers: Dodrecht, The Netherlands, 1999; Chapter 8.

(5) Christensen, R. L.; Goyette, M.; Gallagher, L.; Duncan, J.; DeCoster, B.; Lugtenburg, J.; Jansen, F. J.; van der Hoef, I. *J. Phys. Chem. A* **1999**, *103*, 2399.

(6) Sashima, T.; Koyama, Y.; Yamada, T.; Hashimoto, H. *J. Phys. Chem. B* **2000**, *104*, 5001.

(7) Gradinaru, C. C.; Kennis, J. T. M.; Papagiannakis, E.; van Stokkum, I. H. M.; Cogdell, R. J.; Fleming, G. R.; Niederman, R. A.; van Grondelle, R. *Proc. Natl. Acad. Sci. U.S.A* **2001**, *98*, 2364.

(8) Macpherson, A. N.; Arellano, J., B.; Fraser, N. J.; Cogdell, R. J.; Gillbro, T. *Biophys. J.* **2001**, *80*, 923.

(9) Zhang, J.-P.; Fujii, R.; Qian, P.; Inaba, T.; Mizoguchi, T.; Koyama, Y.; Onaka, K.; Watanabe, Y. *J. Phys. Chem B* **2000**, *104*, 3683.

(10) Croce, R.; Müller, M. G.; Bassi, R.; Holzwarth, A. R. *Biophys. J.* **2001**, *80*, 901.

(11) Krueger, B. P.; Lampoura, S. S.; van Stokkum, I. H. M.; Papagiannakis, E.; Salverda, J. M.; Gradinaru, C. C.; Rutkauskas, D.; Hiller, R. G.; van Grondelle, R. *Biophys. J.* **2001**, *80*, 2843.

(12) Hörvin Billsten, H.; Herek, J. L.; Garcia-Asua, G.; Hashøj, L.; Polívka, T.; Hunter, C. N.; Sundström, V. *Biochemistry* **2002**, *41*, 4127.

(13) Scholes, G. D.; Harcourt, R. D.; Fleming, G. R. *J. Phys. Chem. B* **1997**, *101*, 7302.

(14) Krueger, B. P.; Scholes, G. D.; Fleming, G. R.; *J. Phys. Chem. B* **1998**, *102*, 5378.

(15) Damjanovic, A.; Ritz, T.; Schulten, K. *Phys. Rev. E* **1999**, *59*, 3293.

(16) Damjanovic, A.; Ritz, T.; Schulten, K. *Biophys. J.* **2000**, *79*, 1695.

(17) Hsu, C.-P.; Walla, P. J.; Head-Gordon, M.; Fleming, G. R. *J. Phys Chem. B* **2001**, *105*, 11016.

(18) Frank, H. A.; Desamero, R. Z. B.; Chynwat, V.; Gebhard, R.; van der Hoef, I.; Jansen, F. J.; Lugtenburg, J.; Gosztola, D.; Wasielewski, M. R. *J. Phys. Chem. A* **1997**, *101*, 149.

(19) Sashima, T.; Shiba, M.; Hashimoto, H.; Nagae, H.; Koyama, Y. *Chem. Phys. Lett*. **1998**, *290*, 36.

(20) Sashima, T.; Koyama, Y.; Yamada, T.; Hashimoto, H. *J. Phys. Chem B* **2000**, *104*, 5011.

(21) Fujii, R.; Onaka, K.; Kuki, M.; Koyama, Y.; Watanabe, Y. *Chem. Phys. Lett*. **1998**, *288*, 847.

(22) Frank H. A.; Bautista J. A.; Josue J. S.; Young A. J. *Biochemistry* **2000**, *39*, 2831.

(23) Fujii, R.; Ishikawa, T.; Koyama, Y.; Taguchi, M.; Isobe, Y.; Nagae, H.; Watanabe, Y. *J. Phys. Chem. A* **2001**, *105*, 5348.

(24) Polívka, T.; Herek, J. L.; Zigmantas, D.; Åkerlund, H.-E.; Sundström, V. *Proc. Natl. Acad. Sci. U.S.A.* **1999**, *96*, 4914.

(25) Polívka, T.; Zigmantas, D.; Frank, H. A.; Bautista, J. A.; Herek, J. L.; Koyama, Y.; Fujii, R.; Sundström, V. *J. Phys. Chem. B* **2001**, *105*, 1072.

(26) Krueger, B. P.; Yom, J.; Walla, P. J.; Fleming, G. R. *Chem. Phys. Lett.* **1999**, *310*, 57.

(27) Walla, P. J.; Linden, P. A.; Hsu, C.-P.; Scholes, G. D.; Fleming, G. R. *Proc. Natl. Acad. Sci. U.S.A.* **2000**, *97*, 10808.

(28) Walla, P. J.; Linden, P. A.; Ohta, K.; Fleming, G. R. *J. Phys. Chem. A* **2002**, *106*, 1909.

(29) Polívka, T.; Zigmantas, D.; Sundström, V.; Formaggio, E.; Cinque, G.; Bassi, R. *Biochemistry* **2002**, *41*, 439.

(30) Sundström, V.; Pullerits, T.; van Grondelle, R.; *J. Phys. Chem. B*, **1999**, *103*, 2327.

(31) McDermott, G.; Prince, S. M.; Freer, A. A.; Hawthornwaite-Lawless, A. M.; Papiz, M. Z.; Cogdell, R. J.; Isaacs, N. W. *Nature* **1995**, *374*, 517.

(32) Prince, S. M.; et al. Unpublished data.

(33) Walz, T.; Jamieson, S. J.; Bowers, C. M.; Bullough, P. A.; Hunter, C. N. *J. Mol. Biol.* **1998**, *282*, 833.

(34) Desamero, R. Z. B.; Chynwat, V.; van der Hoef, I.; Jansen, F. J.; Lugtenburg, J.; Gosztola, D.; Wasielewski, M. R.; Cua, A.; Bocian, D. F.; Frank, H. A. *J. Phys. Chem. B* **1998**, *102*, 8151.

(35) Andersson, P.-O.; Bachilo, S. M.; Chen, R.-L.; Gillbro, T. *J. Phys. Chem.* **1995**, *99*, 16199.

(36) Ricci, M.; Bradforth, S. E.; Jimenez, R.; Fleming, G. R. *Chem. Phys. Lett.* **1996**, *259*, 381.

(37) Noguchi, T.; Hayashi, H.; Tasumi, T. *Biochim. Biophys. Acta* **1990**, *1017*, 280.

(38) Fraser N. J.; Dominy, P. J.; Ücker, B.; Siminin, I.; Scheer, H.; Cogdell, R. J. *Biochemistry* **1999**, *38*, 9684.

(39) Frank, H. A.; Bautista, J. A.; Josue, J.; Pendon, Z.; Hiller, R. G.; Sharples, F. P.; Gosztola, D.; Wasielewski, M. R. *J. Phys. Chem. B* **2000**, *104*, 4569.

(40) Zhang, J.-P.; Inaba, T.; Watanabe, Y.; Koyama, Y. *Chem. Phys. Lett.* **2001**, *340*, 484.

(41) Jeevarajan, J. A.; Wei, C. C.; Jeevarajan, A. S.; Kispert, L. D. *J. Phys. Chem.* **1996**, *100*, 5637.

(42) Bally, T.; Roth, K.; Tang, W.; Schrock, R. R.; Knoll, K.; Park, L. Y. *J. Am. Chem. Soc*. **1992**, *114*, 2440.

(43) Spheroidene radical in methanol solution was generated using 8 ns laser pulses centered at 355 nm. The spectrum shown in Figure 8 was reconstructed from kinetics measured in the 800−1100 nm region and each point represents integration over delay times 18−24 μs.

(44) Konovalova, T. A.; Kispert, L. D.; Konovalov, V. *J. Phys. Chem. B* **1997**, *101*, 7858.

(45) Mortensen, A.; Skibsted, L. H. *Free Rad. Res.* **1997**, *26*, 549.

(46) Hanley, J.; Deligiannakis, Y.; Pascal, A.; Faller, P. Rutherford, A. W. *Biochemistry* **1999**, *38*, 8189.

(47) Mortensen, A.; Skibsted, L. H.; Sampson, J.; Rice-Evans, C.; Everett, S. A. *FEBS Lett.* **1997**, *418*, 91.

(48) Zhang, J.-P.; Fujii, R.; Koyama, Y.; Rondonuwu F. S.; Watanabe, Y.; Mortensen, A.; Skibsted, L. H.; *Chem. Phys. Lett.* **2001**, *348*, 235.

(49) Papagiannakis, E.; Kennis, J. T. M.; van Stokkum, I. H. M.; Cogdell, R. J.; van Grondelle, R. *Proc. Natl. Acad. Sci. U.S.A.* **2002**, *99*, 6017.

(50) Becke, A. D. *J. Chem. Phys.* **1993**, *98*, 5648.

(51) Frisch, M. J.; Trucks, G. W.; Schlegel, H. B.; Scuseria, G. E.; Robb, M. A.; Cheeseman, J. R.; Zakrzewski, V. G.; Montgomery, Jr., J. A.; Stratmann, R. E.; Burant, J. C.; Dapprich, S.; Millam, J. M.; Daniels, A. D.; Kudin, K. N.; Strain, M. C.; Farkas, O.; Tomasi, J.; Barone, V.; Cossi, M.; Cammi, R.; Mennucci, B.; Pomelli, C.; Adamo, C.; Clifford, S.; Ochterski, J.; Petersson, G. A.; Ayala, P. Y.; Cui, Q.; Morokuma, K.; Malick, D. K.; Rabuck, A. D.; Raghavachari, K.; Foresman, J. B.; Cioslowski, J.; Ortiz, J. V.; Stefanov, B. B.; Liu, G.; Liashenko, A.; Piskorz, P.; Komaromi, I.; Gomperts, R.; Martin, R. L.; Fox, D. J.; Keith, T.; Al-Laham, M. A.; Peng, C. Y.; Nanayakkara, A.; Gonzalez, C.; Challacombe, M.; Gill, P. M. W.; Johnson, B.; Chen, W.; Wong, M. W.; Andres, J. L.; Gonzalez, C.; Head-Gordon, M.; Replogle, E. S.; Pople, J. A. *Gaussian 98*; Carnegie-Mellon University: Pittsburgh, PA, 1998.

(52) He, Z.; Sundström, V.; Pullerits, T. *Chem. Phys. Lett*. **2001**, *334*, 159.